

### Central European Journal of Chemistry

# Role of temperature in the numerical analysis of CaO under high pressure

**Research Article** 

Purvee Bhardwaj\*, Sadhna Singh

Department of Physics, Barkatullah University, Bhopal 462026, India

Received 18 March 2009; Accepted 3 August 2009

Abstract: In this paper we focus on the elastic and thermodynamic properties of the B1 phase of CaO by using the modified TBP model, including the role of temperature. We have successfully obtained the phase transition pressure and volume change at different temperatures. In addition elastic constants and bulk modulus of B1 phase of CaO at different temperatures are discussed. Our results are comparable with

addition elastic constants and bulk modulus of B1 phase of CaO at different temperatures are discussed. Our results are comparable with the previous ones at high temperatures and pressures. The thermodynamical properties of the B1 phase of CaO are also predicted.

**Keywords:** Oxides • High-pressure • Crystal structure • Mechanical properties • Phase

© Versita Warsaw and Springer-Verlag Berlin Heidelberg.

### 1. Introduction

The lower mantle (670-2890 km depth) is the largest single region of the Earth's interior making up 55% of its volume. As such, it dominates the process of mass, momentum and energy transport in the deep interior and hence may have a substantial influence on the planet's thermal and chemical evolution. Despite a number of analyses made over several years, the major element composition of the lower mantle is still a source of controversy. Until the existence of samples from the lower mantle can be confirmed, comparison between seismological observations and elastic properties of potentially relevant minerals and mineral assemblages represent the most direct way of extracting information regarding the composition and mineralogy of this region. Such comparisons are severely hindered by the lack of sufficient and reliable elasticity data for the relevant phases. The majority of the measurements so far are confined to low pressures so that extrapolations to the extreme conditions corresponding to the lower mantle are needed. Alternatively, the seismic data can be extrapolated to ambient conditions for comparison with laboratory defined mineral properties. These

approaches are usually based on a limited subset of seismic observations such as the density and seismic parameter (or bulk modulus), which are usually known from static compression, shock wave, and ultrasonic experiments.

CaO is a major constituent in the lower mantle [1], and knowing its thermoelasticiy helps us to understand the process of brittle failure, flexure and the propagation of elastic waves [2,3]. However many of its physical properties are still relatively poorly understood. For example, its equation of state (EOS) is relatively well known only at 298K [4-6], while at high pressures and temperatures no experiments are reported. The elastic constants were measure d experimentally at pressures only up to 1 GPa [7] although elasticity data are available over a wide temperature range [8]. Chang and Graham [7] investigated several thermodynamical quantities of CaO at high pressures. The pressure induced phase transition from phase B1 to phase B2 was observed in both diamond cell and shock wave experiments at high pressures ranging from 53 to 70 GPa [4-6,9]. A number of theoretical investigations of structure and phase stability of CaO at high pressures indicate that the B1-B2 phase transition takes place in a wide range

of predicted pressures [10-18]. Correspondingly, first principle computer simulations have been increasingly employed for exploring various properties of the Earths materials under the geophysical relevant conditions. The full potential linear muffin-tin-orbital (FP-LMTO) was used to study the elastic properties and their pressure dependence of four B1-type alkaline earth oxides at high pressures [19]. Recently Karki and Crain [12] have performed plane wave pseudopotential (PPWP) calculations to predict single crystal elastic constants of CaO as a function of pressure up to 140 GPa.

Shanker et al. [20] investigated the theory of thermal expansivity and bulk modulus for MgO, CaO and other minerals in the temperature range 300-1800K using the Gruneisen theory of thermal expansion. Karki et al. investigated the elastic instabilities in crystal (MgO, CaO) from ab-initio stress strain relations [21], vibrational and quasiharmonic thermal properties of CaO under pressure using first principles [22] and structural and elastic properties of MgO periclase were studied up to 150 GPa with the first principle pseudopotential method within the local density approximation [23]. Alfredsson et al. [24] investigated the structural as well as elastic properties and magnetic phase transitions in simple oxides using hybrid exchange functionals within DFT. Yamanaka et al. [25] performed the X-ray powder diffraction measurements of CaO at pressure and temperature of B1-B2 phase transition. Ye Deng et al. [26] investigated the elastic properties of CaO by ab-initio plane wave pseudopotential density functional theory calculation.

Studies of Cohen and Gordon [27] were based on two body potentials and could not explain Cauchy violations ( $C_{12} \neq C_{44}$ ), which are significant in all the divalent metal oxides (DMO). The need of inclusion of three body interaction forces was emphasized by Sims *et al.* [28] for the better matching of results. Thu, it is evident that a realistic model potential for DMO must include the effect of three-body potential (TBP) [29] and van der Waals (vdW) interactions. Tosi and coworkers [30] have demonstrated the significance of van der Waals attraction due to the dipole-dipole (d-d) and dipole-quadrupole (d-q) interactions to depict the cohesion in ionic solids. According to Varshney *et al.* [31], the vdW interactions are the corner stone which are ignored in the first principle calculations.

In the present paper, we used the three body potential model with including the temperature effect. We have studied the phase transition pressure and volume change of CaO at different temperatures. The second order elastic constants (SOECs) which we calculated at T=300 K have been calculated for different pressures. The main aim of this potential is a critical assessment of the performance of this potential in predicting the phase transition and high pressure behavior of CaO.

### 2. Experimental procedure

## 2.1. Potential model and method of calculations

It is well known that pressure causes changes in crystal volume, and consequently it alters the charge distribution of the electron shells. As a result, a deformation of the overlapping electron shells of the adjacent ions takes place, that leads to an increased charge transfer (or three body interaction (TBI) [29]). This interaction becomes more important to consider due to the decrease in interionic spacing of the lattice crystal when pressure gets increased and when ions experience sufficient overlap. This overlapping leads to the transfer (or exchange) of charge. Besides, enhance in overlap energy, the transferred charge due to overlap in electron shells, modifies the coulomb energy by (1+(2n/z) f(r)), where n and z are the number of electrons in outermost shell and ionic charge of compound. The f(r) is the TBI parameter and dependent on the nearest neighbor distance (r) [29]

$$f(r) = f_0 \exp(-r/\rho) \tag{1}$$

The effect of TBI is introduced in the expressions of Gibbs free energy (G = U+PV-TS), in order to obtain the stability condition for a crystal structure. Here, U is the internal energy, which at 0 K is equivalent to the lattice energy, and S is the entropy. Since the theoretical calculations are done at 0 K, the Gibbs free energy is equivalent to enthalpy (H). This is not the realistic approach because experiments are carried out at room temperature. This fact causes discrepancy in comparability of theoretical results with experimental data. To obtain better comparability the room temperature was taken into account in pressure induced theoretical calculations. The Gibbs free energies for rock salt (B1, real) and CsCl (B2, hypothetical) structures at room temperature 300 K are given by:

$$G_{B1}(r) = U_{B1}(r) + PV_{B1}(r) - TS_1$$
 (2)

$$G_{B2}(r') = U_{B2}(r') + PV_{B2}(r') - TS_2$$
 (3)

With  $V_{B1}$  (=2.00r³) and  $V_{B2}$  (=1.54r¹³) as unit cell volumes,  $S_1$  and  $S_2$  are the entropies for  $B_1$  and  $B_2$  phases, respectively. The difference in free energy between two phases

$$\Delta G = \Delta H - T \Delta S \tag{4}$$

should approach to zero. It is a condition for a phase transition.

The first terms in Eqs. 2 and 3 are lattice energies for B<sub>1</sub> and B<sub>2</sub> structures and they are expressed as:

$$U_{B_{i}}(r) = \frac{-\alpha_{m}z^{2}e^{2}}{r} - \frac{(12\alpha_{m}ze^{2}f_{m}(r))}{r} - \left[\frac{C}{r^{6}} + \frac{D}{r^{8}}\right] + 6b\beta_{y} \exp[(r_{i} + r_{j} - r)/\rho + 6b\beta_{y} \exp[(2r_{i} - 1.414r)/\rho] + 6b\beta_{y} \exp[(2r_{j} - 1.414r)/\rho] + (0.5)h\langle\omega^{2}\rangle^{1/2}B_{i}$$
(5)

$$U_{B2}(r') = \frac{-\alpha'_{m} z^{2} e^{2}}{r'} - \frac{(16\alpha'_{m} z e^{2} f_{m}(r'))}{r'} - \left[\frac{C'}{r'^{6}} + \frac{D'}{r'^{8}}\right] + 8b\beta_{ij} \exp[(r_{i} + r_{j} - r')/\rho] + 3b\beta_{ii} \exp[(2r_{i} - 1.154r')/\rho] + 3b\beta_{ij} \exp[(2r_{j} - 1.154r')/\rho] + (0.5)h\langle\omega^{2}\rangle^{1/2}_{B_{2}}$$
(6)

Where  $\alpha_m$  and  $\alpha'_m$  are the Madelung constants for NaCl and CsCl structure respectively. C (C') and D (D') are the overall van der Waals coefficients of B1 (B2) phases,  $\beta_{ij}$  (i,j=1,2) are the Pauling coefficients. Ze is the ionic charge and b ( $\rho$ ) are the hardness (range) parameters, r(r') are the nearest neighbor separations for NaCl (CsCl) structure  $f_m(r)$  is the modified three body force parameter which includes the covalency effect with three body interaction;  $r_i$  ( $r_j$ ) are the ionic radii of ions i (j).  $S_1$  and  $S_2$  are the entropies and  $<\omega^2>^{1/2}$  is the mean square frequency related to the Debye temperature ( $\theta_D$ ) as

$$<\omega^2>^{1/2}=k\theta_D/h \tag{7}$$

here,  $\theta_{D}$  can be expressed by well known Blackman's formula described in [14]

$$\theta_{\rm D} = (h/k) [(5rB_{\rm T})/\mu]^{1/2}$$
 (8)

where  $\boldsymbol{B}_{\scriptscriptstyle T}$  and  $\boldsymbol{\mu}$  are the bulk modulus and reduced mass of the compound.

The first terms in Eqs. 5 and 6 are long range Coulomb energies, second terms appear due to three body interactions corresponding to the nearest neighbor separation r(r') for B1 (B2) phases; third terms appear due to vdW interaction, fourth terms are the energies of the overlap repulsion represented by Born-Mayer potentials for (i,j) ions, fifth and sixth terms are the overlap repulsive terms extended up to the second neighbor ions by using Hafemeister and Flygare (HF) type potential. Seventh term indicates the zero point energy effect and the last term indicate the room and higher temperature effect. Now the entropy

differences in the last term of Eqs. 5 and 6 can be calculated from the relation used in our earlier work [32]:

$$S_1 - S_2 = \int_1^2 \left[ \frac{C_1 - C_2}{T} \right] \tag{9}$$

where, 1 and 2 stand for the B1 and B2 phases,  $C_1$  and  $C_2$  are the specific heats of the two phases at constant pressure, their values can be calculated knowing Gruneisen parameter ( $\gamma$ ) and linear isothermal temperature coefficients ( $\beta$ ):

$$C_i = \frac{\{\beta V_i(B_T)\}_i}{\gamma_i} \tag{10}$$

Gruneisen parameter ( $\gamma$ ) can be calculated with well known formula as follows [33]

$$\gamma = -r_0 / 6 [U'''(r_0) / U''(r_0)] = -r_0 / 6 \rho$$
 (11)

In order to access the relative merit of the present potential, we have calculated the compressibility ( $\beta$ ), molecular force constant (f), infrared absorption frequency ( $u_0$ ), Debye temperature ( $\theta_D$ ), which are directly derived from the cohesive energy,  $\Phi$ (r). Their expressions [34] are given below for reference.

The compressibility is well known to be given by

$$\beta = \frac{3Kr_0}{f} \tag{12}$$

in terms of molecular force constants

$$f = \frac{1}{3} \left[ \phi_{kk'}^{SR}(r) + \frac{2}{r} \phi_{kk'}^{SR}(r) \right]_{r=r_0}$$
 (13)

where  $\Phi_{kk'}^{SR}(r)$  is the short range nearest neighbor (k $\neq$ k') part of  $\Phi$  (r) given by the last three terms in Eqs. 3 and 4. Using force constant f and infrared absorption frequency the reduced mass ( $\mu$ ) of the oxide crystals could be calculated:

$$v_0 = \frac{1}{2\pi} \left(\frac{f}{\mu}\right)^{1/2} \tag{14}$$

This frequency gives us the Debye temperature

$$\theta_D = \frac{h \nu_0}{k} \tag{15}$$

where h and k are the Planck and Boltzmann constants, respectively.

### 3. Results and discussion

The Gibb's free energies contain three model parameters [b,  $\rho$ , f(r)]. The values of these parameters have been evaluated using the first and second order space derivatives [35-37] of the cohesive energy (U) expressed after choosing an appropriate value of  $\rho$  as:

$$\left[\frac{dU}{dr}\right]_{r=r_0} = 0$$

$$\left[\frac{d^2U}{dr^2}\right] = 9kr_0B_T$$

The values of input data and model parameters are listed in Table 1 [38]. In order to obtain the structural phase transition, we have followed the technique of minimization. By minimizing  $U_{\rm B_1}(r)$  and  $U_{\rm B_2}(r')$  at different pressures we obtained the interionic separations r and r' associated with minimum energies for  $\rm B_1$  and  $\rm B_2$  phases, respectively. We have evaluated the corresponding  $\rm G_{\rm B_1}(r)$  and  $\rm G_{\rm B_2}(r')$  and their respective differences  $\rm \Delta G$  (=  $\rm G_{\rm B_1}(r)$  -  $\rm G_{\rm B_2}(r')$ ).

As the pressure increases the value of  $\Delta G$  decreases and approaches zero at the transition pressure. Beyond this pressure  $\Delta G$  becomes negative as the phase B2 becomes stable. These differences have been plotted against pressure (P) in Fig.1 for CaO at different temperatures. The phase transition pressures and volume changes obtained from the model are presented in Table 2. The values of volume changes of CaO are compared with Shankar et al. [20] in different temperature ranges. Our values show the same trend. The volume change of CaO is plotted at different temperatures in Fig. 2. Our results are compared with other theoretical data [20]. The solid lines of presented results show the same trend as given in [20]. Also the volume collapses at phase transition pressure for different temperatures have been plotted in Fig. 3 and compared with the theoretical and experimental work of Karki et al. [22]. It is clear from the figure that our values are close to the theoretical and experimental ones [22].

The B1-B2 phase transition was confirmed with increasing and decreasing pressure at several temperatures. The measurement of the B1-B2 transition pressure in NaCl at high temperatures is observed by Li *et al.* [39], using the diamond anvil cell. Also Bassett

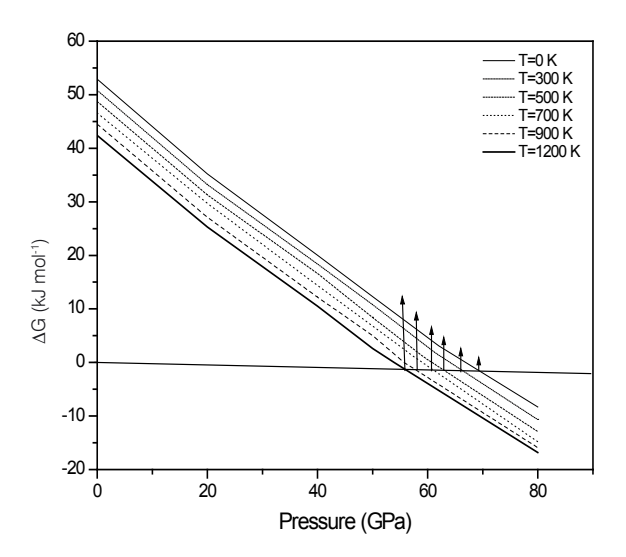


Figure 1. Variation of ΔG (kJ mol<sup>-1</sup>) with pressure for CaO at different temperatures.

et al. [40] studied NaCl by shock wave (Hugoniot) measurements. As temperatures in the shock experiments were estimated to about 1000 K higher than in the static experiments, they concluded that the pressure temperature (P-T) Clapeyron slope of the phase boundary must be negative. As reported by Karki et al. [22] the calculated transition pressure decreases with increasing temperature, thus showing a negative Clapeyron slop. This phase boundary should indeed have a negative slope since the entropy increases across this phase change. Not only the entropy increases but also thermal expansion coefficient (α) and specific heat (C<sub>x</sub>) increase across the transition. The variation of phase transition pressure with temperature is plotted in Fig. 4. It is clear that the phase transition pressure decreases monotonically when the temperature increases. The phase transition pressure becomes smaller 62 GPa (T=0 K), 61.4 GPa (T=300 K), 59.3 GPa (T=500 K), 57.6 GPa (T=700 K), 55.7 GPa (T=900 K) and 54 GPa (T=1200 K) as the temperature increases. Comparison of the pressure-temperature slope obtained in this work and the one described in [22] shows great similarity.

The elasticity of the minerals at high pressure is of substantial physical and geological interest for several reasons. First, our most precise and informative observations of the bulk of the earth are from its elastic properties. Second, the geometry of mantle flow can be clarified by comparing seismological observations of mantle anisotropy with the measured or predicted anisotropy of hypothesized mantle phases. Finally, the elasticity of mineral yields substantial insight into the nature of bonding.

To test the mechanical stability of our model, the elastic properties of proposed materials were computed.

Table 1. Input data and model parameters of the crystal.

Compound	r (Å)	r (Å)	r (Å)	B <sub>⊤</sub> (GPa)	b (10 <sup>-12</sup> ergs)	ρ (Å)	f (r)
CaO	1.06ª	1.40ª	2.405ª	110 <sup>b</sup>	7.52	0.925	-0.624
a[38]: b[6]							

Also, we could reproduce the correct sign of the elastic constants  $(C_{11}-C_{12})$  and  $C_{44}$ .  $C_{11}$  represents a measure of resistance to deformation by a stress applied on (1,0,0) plane with polarization in the direction <100>. C<sub>44</sub> represents the measure of resistance to deformation with respect to shearing stress applied across the (1,0,0) plane with polarization in the <010> direction. The elastic constant C<sub>11</sub> represents elasticity in length. A longitudinal strain produces a change in C<sub>11</sub>. The elastic constants C<sub>12</sub> and C<sub>44</sub> are related to the elasticity in shape, which is a shear constant. A transverse strain causes a change in shape without a change in volume. Therefore,  $C_{12}$  and  $C_{44}$  are less sensitive to pressure as compared to  $C_{11}$ . As pressure increases  $C_{11}$ ,  $C_{12}$  and B (bulk modulus) of the B1 phase at zero temperature increase, but C<sub>44</sub> decreases monotonically.

The values of second order elastic constants (SOEC,s) at different pressures (at T=300 K) are given in Table 3. The variation of SOEC,s with pressure are plotted in Fig. 5. Table 3 and Fig. 5 show that in case of CaO  $\rm C_{11}$  varies largely under the effect of pressure as compared to the variations in the  $\rm C_{12}$  and  $\rm C_{44}$ .

Besides thermo physical properties of CaO at T=300 K were calculated and listed in Table 4. The thermo physical properties provide us the interesting

information about the substance. The Debye characteristic temperature  $\theta_{\rm D}$  reflects its structure stability, the bonds strength between its separate elements, structure defects availability (dislocations in crystalline structure of mineral grains, pores, micro cracks) and its density. Compressibility is used in the earth science to quantify the ability of a soil or rock to reduce in volume with applied pressure. Thermo physical properties have been computed with the help of model parameters and input data listed in Tables 1-3. the bulk modulus at T=300K has been compared to the experimental [8] and other theoretical results [22].

### 4. Conclusions

There is reasonably good agreement of the proposed modified model with the results of other theoretical data [20]. The success achieved in the present investigation can be ascribed to the realistic approach of our model. The charge transfer effect seems to be of great importance at high pressure when the inter-ionic separation reduces considerably and the coordination number increases.

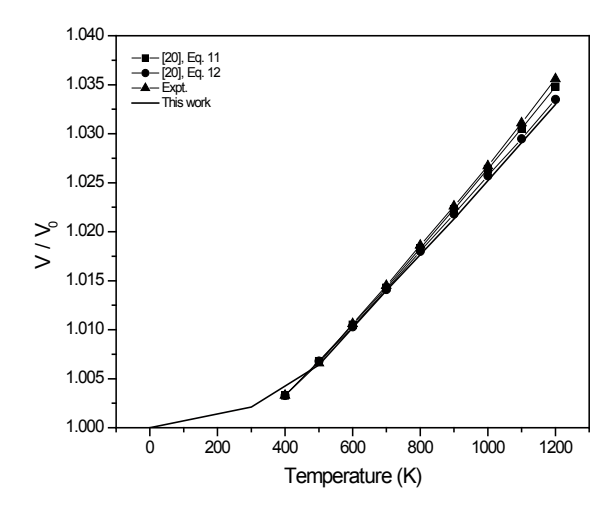
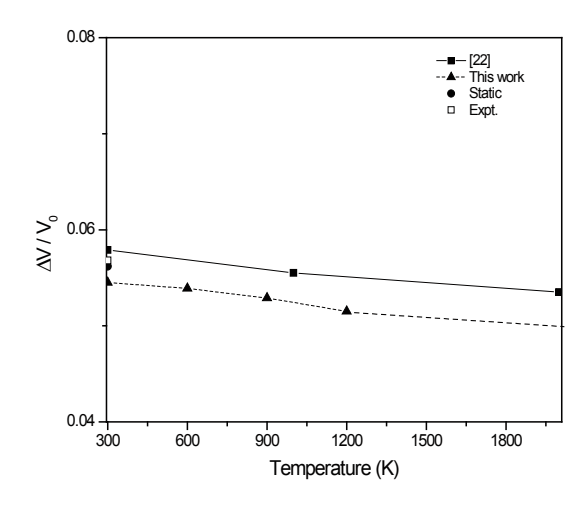


Figure 2. Variation of volume change  $V_p/V_0$  with temperature.



**Figure 3.** Variation of  $\Delta V/V_0$  with temperature.

**Table 2.** Phase Transition pressure and volume change at different temperatures.

Temperature (K)	Phase transition pressure (GPa)	Volume change (V/V <sub>o</sub> )
0 (Present) (Others) (Expt.)	62 56ª 53-70 <sup>b</sup>	1.0000 1.0000 <sup>d</sup> 1.0000 <sup>b</sup>
300 (Present) (Others)	61.4 60°	1.0027 1.0033 <sup>d</sup> ,1.0033°, 1.0033 <sup>f</sup>
500 (Present) (Others)	59.3 -	1.00589 1.00681 <sup>d</sup> , 1.0068 <sup>e</sup> , 1.0066 <sup>f</sup>
700 (Present) (Others)	57.6 -	1.0105 1.0143 <sup>d</sup> , 1.0141°, 1.0145 <sup>f</sup>

 $<sup>^{</sup>a}[22]; ^{b}[4-6]; ^{c}[25]; ^{d}[20], Eq. 11; ^{e}[20], Eq. 12; ^{f}[20], Expt.$ 

60 - This work [22] 55 - 50 - 50 - This work [22] 50 - This work [22] 50 - Temperature (K)

Figure 4. Variation of transition pressure with temperature.

Table 3. Elastic constants at T=300 K of CaO.

P	C <sub>11</sub>	C <sub>12</sub>	<b>C</b> <sub>44</sub>
0	215.13	66.94	77.82
20	393.21	91.85	76.49
40	562.65	116.74	71.49
60	721.04	140.21	64.97
61	728.39	141.26	64.56
62	739.31	145.5	64.35
63	747.69	147.01	63.85
54	753.07	145.68	63.4
65	763.07	148.94	63.07
70	803.84	155.76	61.09
75	843.02	162.42	59.1
80	881.68	167.63	56.78
100	1037.7	194	47.46

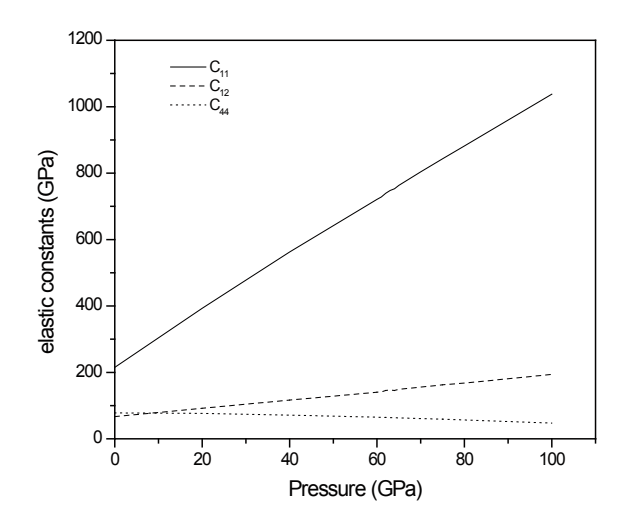


**Figure 5.** Variation of elastic constants with pressure at T=300 K.

Table 4. Thermal properties of CaO at temperature T=300 K

Compound	B <sub>T</sub>	f (10⁴dyn cm⁻¹)	θ <sub>D</sub> (K)	υ <sub>ο</sub> (10¹² Hz)
CaO	116.33	2.1630	682.67	6.749645
(Present)	121 <sup>a</sup>	-	-	-
(Others) (Expt.)	111 <sup>b</sup> , 115 <sup>b</sup>	-	-	-

<sup>&</sup>lt;sup>a</sup>[22]; <sup>b</sup>[8]

Finally, it may be concluded that the present modified three body potential model (MTBP) is suitable for describing the phase transition phenomena and elastic properties of CaO. The inclusion of three body interactions with temperature effect has improved the prediction of phase transition pressures over those obtained from the two-body potential and TBI without temperature effect.

#### References

- [1] T. Yamanaka, K. Kittaka, T. Nagai, J. Mineral. Petrol. Sci. 97, 144 (2002)
- [2] J.B. Hu, Y.Y. Yu, D.C. Dai, H. Tan, Acta Phys. Sin. 54, 5750 (2005)
- [3] Y.M. Tao, H.X. Cao, Q. Jiang, Acta Phys. Sin. 54, 274 (2005)
- [4] R. Jeanloz, T.J. Ahrens, H.K. Mao, P.M. Bell, Science 206, 829 (1979)
- [5] J.F. Mammone, H.K. Mao, P.M. Bell, Geophys. Res. Lett. 8, 140 (1981)
- [6] P. Richet, H.K. Mao, P.M. Bell, Geophys. Res. Lett. 93, 15279 (1988)
- [7] Z.P. Chang, K.E. Graham, J. Phys. Chem. Solids 38, 1355 (1977)
- [8] H. Oda, O.L. Anderson, D.G. Isaak, I. Suzuki, Phys. Chem. Miner. 19, 96 (1992)
- [9] R. Jeanloz, T.J. Ahrens, Geophys. J. R. Astron. Soc. 62, 505 (1980)
- [10] M. Catti, Phys. Rev. B 68, 100101 (2003)
- [11] A. Aguado, L. Bernasconi, P.A. Madden, J. Chem. Phys. 118, 5704 (2003)
- [12] B.B. Karki, J. Crain, J. Geophys. Res. 103, 12405 (1998)
- [13] G. Kalpana, B. Palanivel, M. Rajagopalan, Phys. Rev. B 52 4 (1995)
- [14] H. Zhang, M.S.T. Bukowinski, Phys. Rev. B 44, 2495 (1991)
- [15] M.J. Mehl, R.E. Cohen, H. Krakauer, J. Geophys. Res. 93, 8009 (1988)
- [16] M.J. Mehl, R.J. Hemley, L.L. Boyer, Phys. Rev. B 33, 8685 (1986)
- [17] M.S.T Bukowinski, Geophys. Res. Lett. 12, 536 (1985)
- [18] A.J. Cohen, R.J. Gordon, Phys. Rev. B 14, 4593 (1976)
- [19] T. Tsuchiya, K. Kawamura, J. Chem. Phys. 114, 10086 (2001)
- [20] J. Shanker, S.S. Kushwah, P. Kumar, Physica B 233, 78 (1997)
- [21] B.B. Karki, G.J. Ackland, J. Crain, J. Physics Condensed Matter 9, 8579 (1997)

### **Acknowledgments**

We are thankful to the referees for their valuable comments that have been used for revising the manuscript. The authors are grateful to the Madhya Pradesh Council of Science and Technology (MPCST), Bhopal for their financial. One of authors (PB) is thankful to MPCST for the fellowship.

- [22] (a) B.B. Karki, R.M. Wentzcovitch, Phys. Rev. B 68, 224304 (2003); (b) B.B. Karki, R.M. Wentzcovitch, S. Baroni, Science 286, 1705 (1999); B.B. Karki, R.M. Wentzcovitch, S. Baroni, Phys. Rev. B 61, 8793 (2000)
- [23] B.B. Karki, L. Stixrude, S.J. Clark, M.C. Warren, G.J. Ackland, J. Crain, American Minneralogist 82, 51 (1997)
- [24] M. Alfredsson et al., Mol. Simul. 31, 367 (2005)
- [25] T. Yamanaka, K. Kittaka, T. Nagai, J. Mineral. Petrol. Sci. 97, 144 (2002)
- [26] Y. Deng, O.-H. Jia, X.-R. Chen, J. Zhu, Physica B 392, 229 (2007)
- [27] A.J. Cohen, R.G. Gordon, Phys. Rev. B 12, 3228 (1975)
- [28] C.E. Sims, G.D. Barrera, N.L. Allan, Phys. Rev. B 57, 11164 (1998)
- [29] R. K Singh, Phys. Reports 85, 259 (1982)
- [30] (a) M.P. Tosi, F.G. Fumi, J. Phys. Chem. Solids 23, 359 (1962); (b) M.P. Tosi, Solid State Physics 16, 1 (1964)
- [31] D. Varshney, N. Kaurav, R. Kinge, R.K. Singh, High Pressure Research 25, 145 (2005)
- [32] A. Gaur, S. Singh, R.K. Singh, J. Alloys Compd. 468, 438 (2008)
- [33] J. Shanker, W.N. Bhende, Phys. Stat. Sol. 136, 11 (1986)
- [34] (a) R.K. Singh, N.K. Gaur, Physica B 150, 385 (1988); (b) R.K. Singh, N.K. Gaur, Phys. Rev. B 39, 671 (1989)
- [35] (a) P. Bhardwaj, S. Singh, N.K. Gaur, Mat. Res. Bull. 44, 1366 (2009); (b) P. Bhardwaj, S. Singh, N.K. Gaur, J. of Molecular Structure: THEOCHEM, 897, 95 (2009)
- [36] R.K. Singh, S. Singh, Phys. Rev. B 45, 1019 (1992)
- [37] R.K. Singh S. Singh, Phase Transition 15, 127 (1989)
- [38] D.R. Lide (Ed), CRC Handbook of Chemistry and Physics, 76th edition (CRC Press Inc., Boca Raton, FL, 1995-1996) 21

[39] X. Li and R. Jeanloz, Phys. Rev. B 36, 474 (1987)[40] W.A Bassett, T. Takahashi, H.K. Mao, J.S. Weaver, J. Appl. Phys. 39, 319 (1968)